

RADIATIVE AND ELECTROWEAK RARE B DECAYS

M. NAKAO

KEK, High Energy Accelerator Research Organization, 1-1 Oho, Tsukuba, Ibaraki 305-0801, JAPAN

E-mail: mikihiko.nakao@kek.jp

This report summarizes the latest experimental results on radiative and electroweak rare B meson decays. These rare decay processes proceed through the Flavor-Changing-Neutral-Current processes, and thus are sensitive to the postulated new particles in the theories beyond the Standard Model. Experiments at e^+e^- colliders, Belle, BaBar and CLEO, have been playing the dominant role, while the CDF and D0 experiments have just started to provide new results from Tevatron Run-II. The most significant achievement is the first observation of the decay $B \rightarrow K^*\ell^+\ell^-$, which opens a new window to search for new physics in B meson decays.

1 Introduction

Rare B meson decays that include a photon or a lepton pair in the final state have been the most reliable window—besides the Cabibbo-Kobayashi-Maskawa (CKM) unitarity triangle—to understand the framework of the Standard Model (SM) using the rich sample of B decays, and to search for physics beyond the SM. Belle has just reported that the CP-violating phase in $B \rightarrow \phi K_S^0$ may deviate largely from the SM expectation measured using the $B \rightarrow J/\psi K_S^0$ and related modes.¹ The former is the $b \rightarrow s\bar{s}s$ transition which proceeds presumably through the loop (penguin) diagram for the $b \rightarrow s$ Flavor-Changing-Neutral-Current (FCNC) process, while the latter is the $b \rightarrow c\bar{c}s$ transition which is dominated by the tree diagram and is unlikely to be interfered with by new physics with a large effect. It is therefore an urgent question whether we can also find a similar deviation from the SM in any other related $b \rightarrow s$ transitions using the large samples of $e^+e^- \rightarrow \Upsilon(4S) \rightarrow B\bar{B}$ data available from two B -factories, Belle and BaBar, in order to investigate the nature of the possible new physics signal.

Radiative B decays with a high energy photon in the final state are a unique probe to explore inside the B meson. In the SM, the high energy photon is radiated through FCNC processes, $b \rightarrow s\gamma$ and

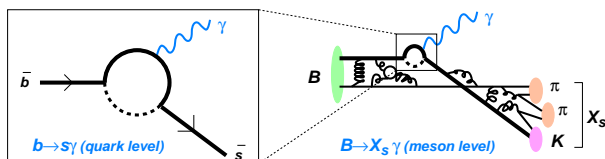


Figure 1. $b \rightarrow s\gamma$ and $B \rightarrow X_s\gamma$.

$b \rightarrow d\gamma$. These transitions are forbidden at the tree level and only proceed via penguin loops formed by a virtual top quark and a W boson, or other higher order diagrams. The loop diagram can also be formed by postulated heavy particles if they exist, and is therefore sensitive to physics beyond the SM. The $b \rightarrow s\gamma$ decay rate is large enough to have been measured already by CLEO² and ALEPH,³ and then by Belle⁴ and BaBar.^{5,6} As illustrated in Fig. 1, the $b \rightarrow s\gamma$ transition at the quark level can be studied by performing an inclusive measurement for $B \rightarrow X_s\gamma$, where X_s is an inclusive state with a strangeness $S = \pm 1$. The photon energy spectrum, which can be characterized by its mean energy and moments, provides a useful constraint to the heavy quark effective theory that essentially helps to reduce the uncertainties in the inclusive semi-leptonic B decay rates and hence the extraction of $|V_{cb}|$ and $|V_{ub}|$. In contrast to the inclusive studies, exclusive decay modes such as $B \rightarrow K^*\gamma$ are experimentally much easier to measure and have been extensively explored. However, one has to always consider large model dependent hadronic uncertainties to compare the results with the SM. Such uncertainties largely cancel by searching for CP- and isospin asymmetries. Though the $b \rightarrow d\gamma$ transition is suppressed by a CKM factor $|V_{td}/V_{ts}|^2 \sim \mathcal{O}(10^{-2})$ with respect to $b \rightarrow s\gamma$, searches are still being pursued for this exclusive decay channel.

Electroweak rare B decays proceeding through a similar FCNC process $b \rightarrow s\ell^+\ell^-$ ($\ell = e, \mu$) involves a virtual photon or weak boson, and has sensitivities to new physics that are not covered by $b \rightarrow s\gamma$. This process is suppressed with respect to $b \rightarrow s\gamma$ by an additional α_{em} factor that has made it inaccessible before the B -factories. Having two leptons

in the final state, one can measure the dependence on the momentum transfer squared $q^2 (= M(\ell^+\ell^-)^2)$ of the virtual γ/Z . Furthermore, measurement of the forward-backward asymmetry of the lepton decay angle will be a unique probe in this electroweak process, with a small theoretical uncertainty even in the exclusive decay $B \rightarrow K^*\ell^+\ell^-$. The pure weak process, $b \rightarrow s\nu\bar{\nu}$ is experimentally extremely difficult.

Pure leptonic decay $B_{d,s}^0 \rightarrow \ell^+\ell^-$ is based on the same quark diagram as $b \rightarrow (d,s)\ell^+\ell^-$, and hence has a similar sensitivity to new physics. The SM expected branching fractions are beyond the current experimental reach, but new physics may dramatically enhance the decay rate, especially for $B_s \rightarrow \mu^+\mu^-$, for which the Tevatron experiments have just restarted to provide new information. The charged counter part, $B^+ \rightarrow \tau^+\nu$ and $B^+ \rightarrow \ell^+\nu$, are tree level processes. These decays have not been observed yet because of the very small branching fractions due to the GIM suppression mechanism and the experimental difficulty due to the missing neutrino.

In this report, the latest results on radiative (Sec. 2), electroweak (Sec. 3) and pure leptonic (Sec. 4) B decays are reviewed. Belle has analyzed up to 140 fb^{-1} corresponding to 152 million $B\bar{B}$ pairs, while BaBar has analyzed up to 113 fb^{-1} corresponding to 123 million $B\bar{B}$ pairs. The first results from the Tevatron Run-II data from CDF and D0 are also included. Finally Sec. 5 concludes this report.

2 Radiative B Decays

2.1 Inclusive $B \rightarrow X_s\gamma$ Branching Fraction

Due to the two-body decay nature of the quark level process of $b \rightarrow s\gamma$, the photon energy spectrum of $B \rightarrow X_s\gamma$ has a peak around half of the b quark mass. This peak is the signature of the fully inclusive $B \rightarrow X_s\gamma$ measurement. On top of this signal, there are huge background sources as shown in Fig. 2. The largest contribution is from the continuum process $e^+e^- \rightarrow q\bar{q}$ ($q = u, d, s, c$) in which copious $\pi^0 \rightarrow \gamma\gamma$ and $\eta \rightarrow \gamma\gamma$ are the sources of high energy photons, and the initial-state radiation process $e^+e^- \rightarrow q\bar{q}\gamma$. These continuum backgrounds are reliably subtracted by using the off-resonance data sample taken slightly below the $\Upsilon(4S)$ resonance. The background from B decay is also signif-

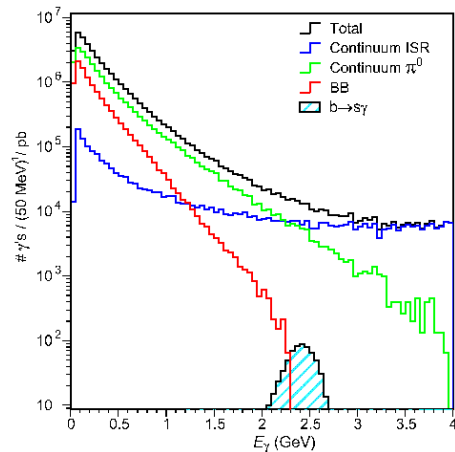


Figure 2. Expected photon energy distribution for $B \rightarrow X_s\gamma$ signal and various background sources.

icant, especially for lower photon energies. To estimate and subtract the B decay background, one has to largely rely on the Monte Carlo simulation. As the signal rate rapidly decreases and the background rate rapidly increases towards lower photon energies, it is inevitable that one requires a minimum photon energy (E_γ^{\min}) and extrapolates the spectrum below E_γ^{\min} to obtain the total branching fraction.

An alternative semi-inclusive method is to sum up all the possible fully reconstructed $X_s\gamma$ final states, where X_s is formed from one kaon and up to four pions. In this case, one can require the kinematic constraints on the beam-energy constrained mass $M_{bc} = \sqrt{E_{\text{beam}}^{*2} - p_B^{*2}}$ (also denoted as the beam-energy substituted mass M_{ES}) and $\Delta E = E_B^* - E_{\text{beam}}^*$, using the beam energy E_{beam}^* and fully reconstructed momentum p_B^* and energy E_B^* of the B candidate in the center-of-mass (CM) frame. Therefore the large backgrounds can be reduced at the cost of introducing an additional error due to the model dependent hadronization uncertainties.

So far, CLEO² and BaBar⁵ have performed the fully inclusive measurement, and Belle⁴ and BaBar⁶ have performed the semi-inclusive measurement. Figure 3 summarizes these results, together with the measurement performed by ALEPH.³ CLEO has applied the lowest E_γ^{\min} of 2.0 GeV and has the smallest error, while BaBar requires $E_\gamma^{\min} = 2.1$ GeV, and Belle requires $M(X_s) < 2.1$ GeV which is roughly equivalent to $E_\gamma^{\min} \sim 2.25$ GeV.

The average of the five measurements, including the two from BaBar with an overlapping data set, has

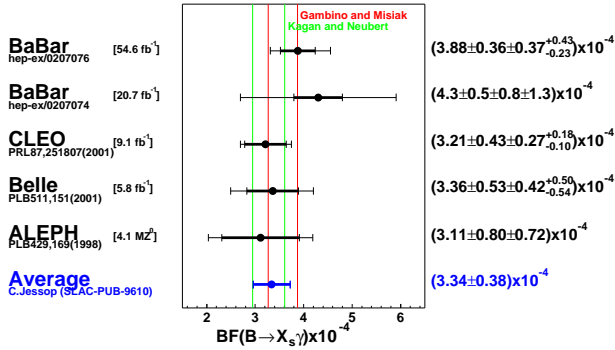


Figure 3. $B \rightarrow X_s \gamma$ branching fraction measurements.

been calculated taking into account the correlation of the systematic and theory errors, as⁷

$$\mathcal{B}(B \rightarrow X_s \gamma) = (3.34 \pm 0.38) \times 10^{-4}. \quad (1)$$

The latest SM calculation⁸ predicts $\mathcal{B}(B \rightarrow X_s \gamma) = (3.57 \pm 0.30) \times 10^{-4}$, in very good agreement with the world average. The prediction fully includes up to Next-to-Leading-Order QCD corrections.⁹

This result can be used to constrain new physics hypotheses.^{8,10,11} For example, any new physics that has only a constructive interference with the SM amplitude is strongly constrained. The Type-II charged Higgs boson is one such example, and its mass has to be greater than 350 GeV if there is no other destructive amplitude.^{8,10} Many SUSY models can, however, have also a destructive amplitude that may cancel the constructive part. The decay amplitude is usually written down using the effective Hamiltonian with Wilson coefficients for the relevant operators. The $B \rightarrow X_s \gamma$ result constrains the magnitude of the C_7 Wilson coefficient, that can be a useful measure of a possible deviation from the SM, and also is an input parameter to the constraints provided by other measurements.

In order to further improve the measurement, it is necessary to lower the minimum photon energy. The latest Belle and BaBar data samples, with the largest off-resonance data size, have yet to be analyzed. A new effort to significantly reduce the theory error by including the Next-to-Next-to-Leading-Order QCD correction has also been started.

2.2 Exclusive $B \rightarrow K^* \gamma$

The measurement of the $B \rightarrow K^* \gamma$ exclusive branching fraction is straightforward, since one can use the M_{bc} , ΔE and K^* mass constraints. (K^* denotes

Table 1. $B \rightarrow K^* \gamma$ branching fractions

	$B^0 \rightarrow K^{*0} \gamma$ [$\times 10^{-5}$]	$B^+ \rightarrow K^{*+} \gamma$ [$\times 10^{-5}$]
CLEO	$4.55 \pm 0.70 \pm 0.34$	$3.76 \pm 0.86 \pm 0.28$
BaBar	$4.23 \pm 0.40 \pm 0.22$	$3.83 \pm 0.62 \pm 0.22$
Belle	$4.09 \pm 0.21 \pm 0.19$	$4.40 \pm 0.33 \pm 0.24$

$K^*(892)$ throughout this report.) The latest Belle measurement (Fig. 4) uses 78 fb^{-1} data, with a total error of much less than 10% for each of the B^0 and B^+ decays. The results from CLEO,¹² BaBar¹³ and Belle¹⁴ are in good agreement and are listed in Table 1. The world averages are calculated as

$$\mathcal{B}(B^0 \rightarrow K^{*0} \gamma) = (4.17 \pm 0.23) \times 10^{-5}, \quad (2)$$

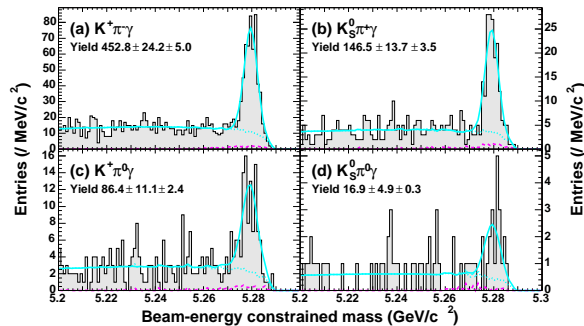
$$\mathcal{B}(B^+ \rightarrow K^{*+} \gamma) = (4.18 \pm 0.32) \times 10^{-5}. \quad (3)$$

The corresponding theoretically predicted branching fraction is about $(7 \pm 2) \times 10^{-5}$, higher than the measurement with a large uncertainty.¹⁵ As the $b \rightarrow s \gamma$ transition is well understood by the inclusive measurement, we consider the deviation is due to the ambiguous hadronic form factor, for which the light-cone QCD sum rule result of $F_7^{B \rightarrow K^*}(0) = 0.38 \pm 0.05$ is used. However, a recent lattice-QCD calculation¹⁶ is suggesting that the expected form-factor is as small as $F_7^{B \rightarrow K^*}(0) = 0.25 \pm 0.04$ and is consistent with the value of $F_7^{B \rightarrow K^*}(0) = 0.27 \pm 0.04$ extracted from the measured branching fraction.

A better approach to exploit the $B \rightarrow K^* \gamma$ branching fraction measurements is to consider isospin asymmetry.¹⁷ A small difference in the branching fractions between $B^0 \rightarrow K^{*0} \gamma$ and $B^+ \rightarrow K^{*+} \gamma$ tells us the sign of the combination of the Wilson coefficients, C_6/C_7 . Belle has taken into account the correlated systematic errors and performed a measurement as

$$\begin{aligned} \Delta_{+0} &\equiv \frac{(\tau_{B^+}/\tau_{B^0})\mathcal{B}(B^0 \rightarrow K^{*0} \gamma) - \mathcal{B}(B^+ \rightarrow K^{*+} \gamma)}{(\tau_{B^+}/\tau_{B^0})\mathcal{B}(B^0 \rightarrow K^{*0} \gamma) + \mathcal{B}(B^+ \rightarrow K^{*+} \gamma)} \\ &= (+0.003 \pm 0.045 \pm 0.018), \end{aligned} \quad (4)$$

which is consistent with zero and one cannot tell whether the SM prediction ($\Delta_{+0} > 0$) is correct yet. Here, the lifetime ratio $\tau_{B^+}/\tau_{B^0} = 1.083 \pm 0.017$ is used, and the B^0 to B^+ production ratio is assumed to be unity. The latter is measured to be $f_0/f_+ = 1.072 \pm 0.057$ and is a source of an additional systematic error.

Figure 4. $B \rightarrow K^* \gamma$ signal from Belle.Table 2. $B \rightarrow K_2^*(1430) \gamma$ branching fractions.

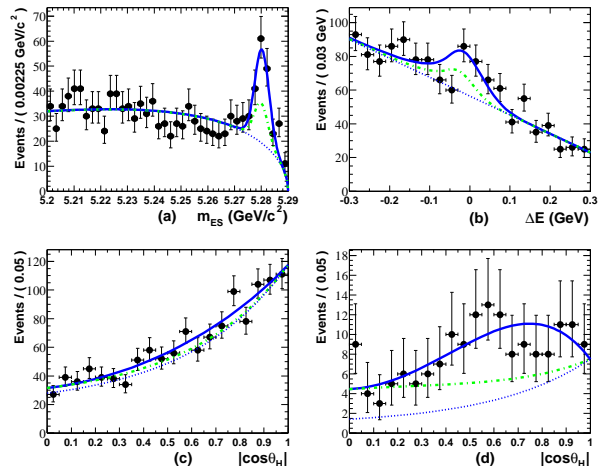
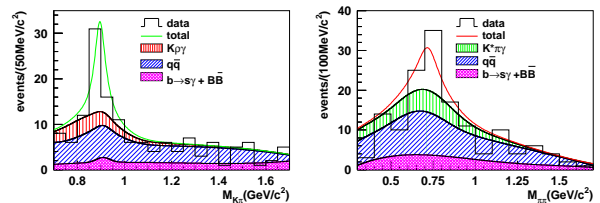
	$B^0 \rightarrow K_2^*(1430)^0 \gamma$ [$\times 10^{-6}$]	$B^+ \rightarrow K_2^*(1430)^+ \gamma$ [$\times 10^{-6}$]
CLEO	$16.6^{+5.9}_{-5.3} \pm 1.3$	—
Belle	$13 \pm 5 \pm 1$	—
BaBar	$12.2 \pm 2.5 \pm 1.1$	$14.4 \pm 4.0 \pm 1.3$

2.3 Other Exclusive Radiative Decays

The dominant radiative decay channel $B \rightarrow K^* \gamma$ covers only 12.5% of the total $B \rightarrow X_s \gamma$ branching fraction, and the rest has to be accounted for by decays with higher resonances or multi-body decays. Knowledge of these decay modes will eventually be useful to reduce the systematic error of the inclusive measurement. Some of the decays have a particular property that is useful to search for new physics. As an example, the decay channel $B^0 \rightarrow K_1(1270)^0 \gamma \rightarrow K_S^0 \rho^0 \gamma$ will be useful to measure the time-dependent CP-asymmetry;¹⁸ while another such measurement is experimentally challenging: $B^0 \rightarrow K^{*0} \gamma \rightarrow K_S^0 \pi^0 \gamma$ using the detached $K_S^0 \rightarrow \pi^+ \pi^-$ decay vertex. Another example is to use the decay $B^+ \rightarrow K_1(1400)^+ \gamma \rightarrow K_S^0 \pi^+ \pi^0$ for a photon polarization measurement.¹⁹

The $B \rightarrow K_2^*(1430) \gamma$ decay mode is unique since the $K_2^*(1430)$ decays into a $K\pi$ combination, while many other resonances have very small or no decay width to $K\pi$. After measurements by CLEO¹² and Belle,²⁰ BaBar has also performed a new measurement²¹ (Fig. 5). Branching fractions are listed in Table 2. The results are in agreement with the SM predictions,²² for example, $(17.3 \pm 8.0) \times 10^{-6}$.

Belle has extended the analysis into multi-body decay channels.²⁰ Using 29 fb^{-1} data, the decay $B^+ \rightarrow K^+ \pi^+ \pi^- \gamma$ is measured to have a branching

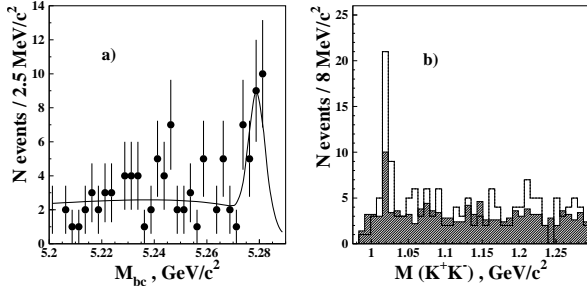
Figure 5. $B^0 \rightarrow K_2^*(1400)^0 \gamma$ signal by BaBar.Figure 6. $B^+ \rightarrow K^{*0} \pi^+ \gamma$ and $B \rightarrow K^+ \rho^0 \gamma$ from Belle.

fraction of $(24 \pm 5 \pm 4) \times 10^{-6}$ for $M(K\pi\pi) < 2.4 \text{ GeV}$. The decay is dominated by $K^{*0} \pi^+ \gamma$ and $K^+ \rho^0 \gamma$ final states that overlap each other as shown in Fig. 6. At this moment, it is not possible to disentangle resonant states that decay into $K^* \pi$ or $K \rho$, such as $K_1(1270)$, $K_1(1400)$, $K^*(1650)$, and so on. A clear $B^+ \rightarrow K^+ \phi \gamma$ (5.5σ) signal was recently observed by Belle with 90 fb^{-1} data (Fig. 7), together with a 3.3σ evidence for $B^0 \rightarrow K_S^0 \phi \gamma$. There is no known $K\phi$ resonant state. This is the first example of a $s\bar{s}s\gamma$ final state. Branching fractions are measured to be²³

$$\begin{aligned} \mathcal{B}(B^+ \rightarrow K^+ \phi \gamma) &= (3.4 \pm 0.9 \pm 0.4) \times 10^{-6} \\ \mathcal{B}(B^0 \rightarrow K^0 \phi \gamma) &= (4.6 \pm 2.4 \pm 0.4) \times 10^{-6} \\ &< 8.3 \times 10^{-6} \quad (90\% \text{ CL}) \end{aligned} \quad (5)$$

With more data, one can perform a time-dependent CP-asymmetry measurement with the $K_S^0 \phi \gamma$ decay channel.

Radiative decays with baryons in the final state have been searched for by CLEO,²⁴ in the $B^- \rightarrow \Lambda \bar{p} \gamma$ channel for photon energies greater than 2 GeV. The analysis is also sensitive to $B^- \rightarrow \Sigma^0 \bar{p} \gamma$ with a

Figure 7. $B^+ \rightarrow K\phi\gamma$ from Belle.

slightly shifted ΔE signal window due to the missing soft photon in $\Sigma^0 \rightarrow \Lambda\gamma$. Upper limits are given as

$$\begin{aligned} \mathcal{B}(B^- \rightarrow \Lambda\bar{p}\gamma) + 0.3\mathcal{B}(B^- \rightarrow \Sigma^0\bar{p}\gamma) &< 3.3 \times 10^{-6} \\ \mathcal{B}(B^- \rightarrow \Sigma^0\bar{p}\gamma) + 0.4\mathcal{B}(B^- \rightarrow \Lambda\bar{p}\gamma) &< 6.4 \times 10^{-6}. \end{aligned} \quad (6)$$

Considering isospin and other resonances such as $N(1232)$, an upper limit on baryonic radiative decay is obtained to be less than 3.8×10^{-5} , or 13% of the total $B \rightarrow X_s\gamma$ branching fraction.

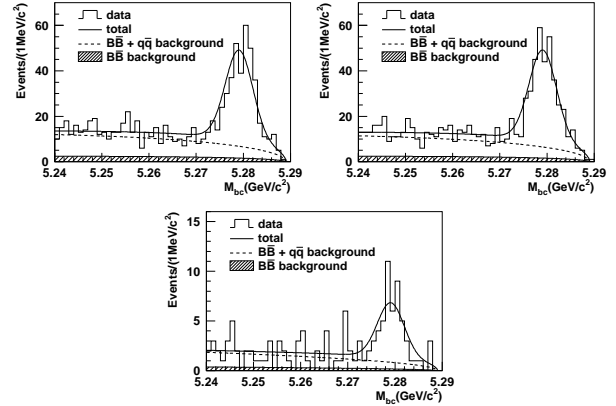
In summary, $(35 \pm 6)\%$ of the total $B \rightarrow X_s\gamma$ is measured to be one of $B \rightarrow K^*\gamma$ (12.5%), $B \rightarrow K_2^*(1430)\gamma$ (4% after excluding $K\pi\pi\gamma$), $B \rightarrow K^*\pi\gamma$ (9%), $B \rightarrow K\rho\gamma$ (9%) or $B \rightarrow K\phi\gamma$ (1%). The remaining $(65 \pm 6)\%$ would be accounted for by decays with multi-body final states, baryonic decays, modes with η and η' , multi-kaon final states other than $K\phi\gamma$ or in the large X_s mass range.

2.4 Search for Direct CP-asymmetry

Direct CP-asymmetry in $B \rightarrow X_s\gamma$ is predicted to be 0.6% in the SM with a small error.^{25,26} This is contrary to the other hadronic decay channels with the $b \rightarrow s$ transition, for which usually larger SM CP-asymmetries are predicted, however, with large uncertainties. Although such a small SM asymmetry is beyond the sensitivity of the current B -factories, many extensions to the SM predict that it is possible to produce a large CP-asymmetry greater than 10%.^{26,27} A large CP-asymmetry will be a clear sign of new physics.

There has been only one measurement by CLEO²⁸ to search for the direct CP-asymmetry of the radiative decays, which is sensitive also to $B \rightarrow X_d\gamma$. The result is expressed as

$$\begin{aligned} 0.965A_{CP}(B \rightarrow X_s\gamma) + 0.02A_{CP}(B \rightarrow X_d\gamma) \\ = (-0.079 \pm 0.108 \pm 0.022) \times (1 \pm 0.030). \end{aligned} \quad (7)$$

Figure 8. \bar{B} -tagged (top-left), B -tagged (top-right) and ambiguous (bottom) $B \rightarrow X_s\gamma$ signal from Belle.

The SM predicts that $B \rightarrow X_d\gamma$ has a much larger A_{CP} with an opposite sign to that of $B \rightarrow X_s\gamma$.

A new $A_{CP}(B \rightarrow X_s\gamma)$ measurement performed by Belle²⁹ uses a similar technique to CLEO's, summing up the exclusive modes of one kaon plus up to four pions. In addition, modes with three kaon plus up to one pion are included. Belle's result eliminates $B \rightarrow X_d\gamma$ by exploiting particle identification devices for the tagged hadronic recoil system. CLEO requires $E_\gamma^{\min} = 2.2$ GeV while Belle require $M(X_s) < 2.1$ GeV which roughly corresponds to $E_\gamma^{\min} \sim 2.25$ GeV. Events are self-tagged as B candidates (B^0 or B^+) or \bar{B} candidates (\bar{B}^0 or B^-), except for ambiguous modes with a K_S^0 and zero net charge. In order to correct the imperfect knowledge of the hadronic final state ingredients, the signal yield for each exclusive mode is used to correct the Monte Carlo multiplicity distribution. The resulting \bar{B} -tagged ($342 \pm 23^{+7}_{-14}$ events), B -tagged ($349 \pm 23^{+7}_{-14}$ events) and ambiguous ($47.8 \pm 8.7^{+1.4}_{-1.8}$ events) signals are shown in Fig. 8. Using the wrong-tag fractions of 0.019 ± 0.014 between B - and \bar{B} -tagged, 0.240 ± 0.192 from ambiguous to B - or \bar{B} -tagged, and 0.0075 ± 0.0079 from B - or \bar{B} -tagged to ambiguous samples, the asymmetry is measured to be

$$A_{CP}(B \rightarrow X_s\gamma) = 0.004 \pm 0.051 \pm 0.038. \quad (8)$$

The result corresponds to a 90% confidence level limit of $-0.107 < A_{CP}(B \rightarrow X_s\gamma) < 0.099$, and therefore already constrains extreme cases of the new physics parameter space.

For exclusive radiative decays, it is straightfor-

Table 3. $B \rightarrow K^*\gamma$ direct CP-asymmetry

CLEO (9.1 fb^{-1})	$(8 \pm 13 \pm 3) \times 10^{-2}$
BaBar (20.7 fb^{-1})	$(-4.4 \pm 7.6 \pm 1.2) \times 10^{-2}$
Belle (78 fb^{-1})	$(-0.1 \pm 4.4 \pm 0.8) \times 10^{-2}$

ward to extend the analysis to search for direct CP-asymmetry.^{12–14} Particle identification devices of Belle and BaBar resolve the possible ambiguity between $K^{*0} \rightarrow K^+\pi^-$ and $\overline{K}^{*0} \rightarrow K^-\pi^+$ to an almost negligible level with a reliable estimation of the wrong-tag fraction (0.9% for Belle). The results of the asymmetry measurements are listed in Table 3, whose average is

$$A_{CP}(B \rightarrow K^*\gamma) = (-0.5 \pm 3.7) \times 10^{-2}. \quad (9)$$

It is usually considered that the large CP-violation in $B \rightarrow K^*\gamma$ is not allowed in the SM and the result may be used to constrain new physics. However, as the strong phase difference involved may not be reliably calculated for exclusive decays, the interpretation may be model dependent.

2.5 Search for $b \rightarrow d\gamma$ Final States

There are various interesting aspects in the $b \rightarrow d\gamma$ transition. Within the SM, most of the diagrams are a copy of those for $b \rightarrow s\gamma$, except for the replacement of the CKM matrix element V_{ts} with V_{td} . A measurement of the $b \rightarrow d\gamma$ process will therefore provide the ratio $|V_{td}/V_{ts}|$ without large model dependent uncertainties. This is in contrast with the current best $|V_{td}/V_{ts}|$ limit obtained from Δm_s and Δm_d in B_s and B_d mixing with the help of lattice QCD calculations. Unfortunately, the inclusive $B \rightarrow X_d\gamma$ measurement is extremely difficult due to its small rate and the huge $B \rightarrow X_s\gamma$ background, and the use of exclusive decay modes such as $B \rightarrow \rho\gamma$ involves other model dependences. If the constraints of the SM is relaxed, it is not necessary to retain the CKM structure, and $b \rightarrow d\gamma$ becomes a completely new probe to search for new physics effects in the $b \rightarrow d$ transition that might be hidden in the B_d mixing and cannot be accessed in the $b \rightarrow s$ transition. This mode is also the place where a large direct CP-asymmetry is predicted within and beyond the SM.

The search for the exclusive decay $B \rightarrow \rho\gamma$ is as straightforward as the measurement of $B \rightarrow K^*\gamma$, except for its small branching fraction, the enormous combinatorial background from copious ρ mesons

Table 4. 90% confidence level upper limits on the $B \rightarrow \rho\gamma$ and $\omega\gamma$ branching fractions.

	$\rho^+\gamma$	$\rho^0\gamma$	$\omega\gamma$
CLEO (9.1 fb^{-1})	13×10^{-6}	17×10^{-6}	9.2×10^{-6}
Belle (78 fb^{-1})	2.7×10^{-6}	2.6×10^{-6}	4.4×10^{-6}
BaBar (78 fb^{-1})	2.1×10^{-6}	1.2×10^{-6}	1.0×10^{-6}

and random pions, and the huge $B \rightarrow K^*\gamma$ background that overlaps with the $B \rightarrow \rho\gamma$ signal window. BaBar has optimized the background suppression algorithm using a neural net technique with input parameters of the event shape, helicity angle and vertex displacement between the signal candidate and the rest of the event, and has optimized the kaon rejection algorithm so that the $B \rightarrow K^*\gamma$ background can be suppressed to a negligible level. $B \rightarrow \omega\gamma$ is not affected by $B \rightarrow K^*\gamma$, but it is still hardly observed. The upper limits obtained by BaBar,³⁰ Belle³¹ and CLEO¹² are summarized in Table 4. The best upper limits by BaBar are still about twice as large as the SM predictions,¹⁵ $(9.0 \pm 3.4) \times 10^{-7}$ for $\rho^+\gamma$, and $(4.9 \pm 1.8) \times 10^{-7}$ for $\rho^0\gamma$ and $\omega\gamma$.

Using the isospin relation $\Gamma(B \rightarrow \rho\gamma) \equiv \Gamma(B^+ \rightarrow \rho^+\gamma) = 2\Gamma(B^0 \rightarrow \rho^0\gamma)$, the combined $B \rightarrow \rho\gamma$ upper limit from BaBar becomes $\mathcal{B}(B \rightarrow \rho\gamma) < 1.9 \times 10^{-6}$. The ratio of the branching fractions can be expressed as

$$\frac{\mathcal{B}(B \rightarrow \rho\gamma)}{\mathcal{B}(B \rightarrow K^*\gamma)} = \left| \frac{V_{td}}{V_{ts}} \right|^2 \left(\frac{m_B^2 - m_\rho^2}{m_B^2 - m_{K^*}^2} \right)^3 \zeta^2 [1 + \Delta R] < 0.047 \text{ (90\% CL)} \quad (10)$$

where $\zeta = 0.76 \pm 0.10$ is the ratio of the form factors obtained from the light-cone QCD sum rule and $\Delta R = 0.0 \pm 0.2$ is to account for $SU(3)$ breaking effects. From this inequality, a bound on V_{td} is given as $|V_{td}/V_{ts}| < 0.34$, which is still a weaker constraint than that given by $\Delta m_s/\Delta m_d$. One can still argue about the validity of the form factor ratio,³² as a recent lattice QCD calculation¹⁶ gives a value of $\zeta = 0.91 \pm 0.08$ that leads to a different constraint on V_{td} as shown in Fig. 9.

3 Electroweak Rare B Decays

The $b \rightarrow s\ell^+\ell^-$ transition has a lepton pair in the final state, which is a clear signature of the decay.

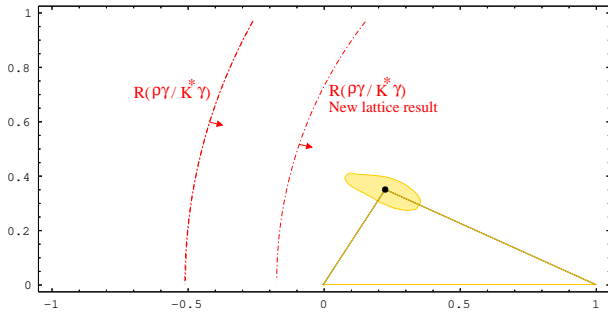


Figure 9. Bound on V_{td} from the ratio of branching fractions of $B \rightarrow \rho\gamma$ to $B \rightarrow K^*\gamma$.

The decay amplitude is written down using three Wilson coefficients, C_7 , C_9 and C_{10} . Although there are three unknown complex coefficients ($|C_7|$ is obtained from $B \rightarrow X_s\gamma$), it is possible to disentangle all of them from measurements of the $\hat{s} = q^2/m_b^2$ dependent branching fraction $d\Gamma/d\hat{s}$ and the forward-backward asymmetry $dA_{FB}/d\hat{s}$,

$$\begin{aligned} \frac{d\Gamma}{d\hat{s}} &= \left(\frac{\alpha_{\text{em}}}{4\pi}\right)^2 \frac{G_F^2 m_b^5 |V_{ts}^* V_{tb}|^2}{48\pi^3} (1 - \hat{s})^2 \\ &\times \left[(1 + 2\hat{s}) (|C_9^{\text{eff}}|^2 + |C_{10}^{\text{eff}}|^2) + 4\left(1 + \frac{2}{\hat{s}}\right) |C_7^{\text{eff}}|^2 \right. \\ &\quad \left. + 12\text{Re}(C_7^{\text{eff}} C_9^{\text{eff}}) \right] + \text{corr.} \end{aligned} \quad (11)$$

$$\frac{dA_{FB}}{d\hat{s}} = C_{10}^{\text{eff}} (2C_7^{\text{eff}} + C_9^{\text{eff}} \hat{s}) / (d\Gamma/d\hat{s}), \quad (12)$$

where QCD corrections are included in the Wilson coefficients.

There are two amplitudes that interfere with $b \rightarrow s\ell^+\ell^-$: one is $b \rightarrow s\gamma$ at $q^2 \rightarrow 0$ and the other is $b \rightarrow (c\bar{c})s$ where $(c\bar{c})$ is a charmonium state such as J/ψ or ψ' that decays into $\ell^+\ell^-$. The latest theory calculation that includes Next-to-Next-to-Leading-Order QCD corrections has been completed for the restricted range of $0.05 < \hat{s} < 0.25$ to avoid these interferences.³³

Similarly to $b \rightarrow s\gamma$, there are a number of extensions to the SM³⁵ that one may be sensitive to by studying $b \rightarrow s\ell^+\ell^-$, and B -factories have just opened the window to search for such effects with a huge sample of B decays that was not available before.

3.1 Observation of $B \rightarrow K^*\ell^+\ell^-$

The first signal of $B \rightarrow K\ell^+\ell^-$ was observed by Belle³⁶ using 29 fb⁻¹ data and confirmed by BaBar³⁷ with 78 fb⁻¹, while the $B \rightarrow K^*\ell^+\ell^-$ signal, which

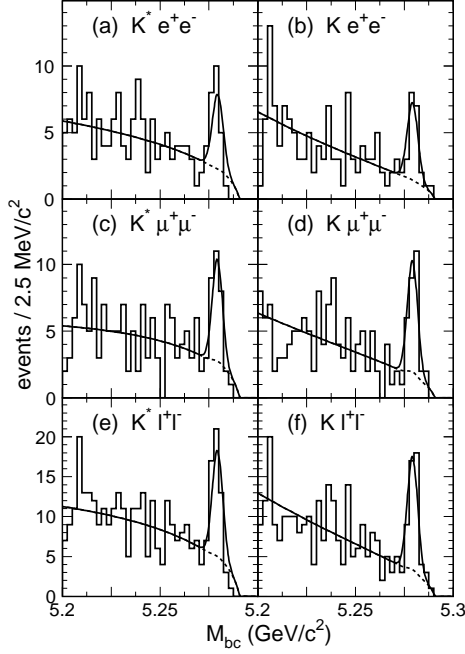
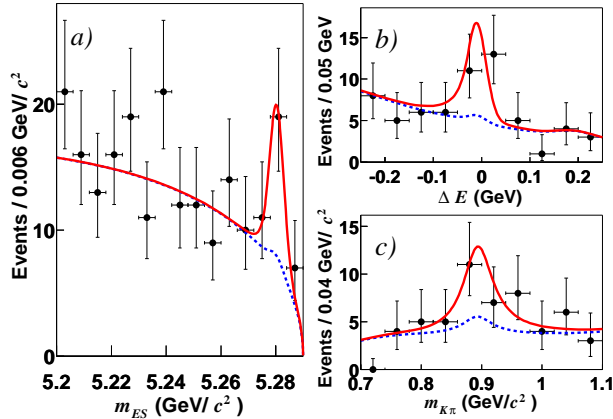
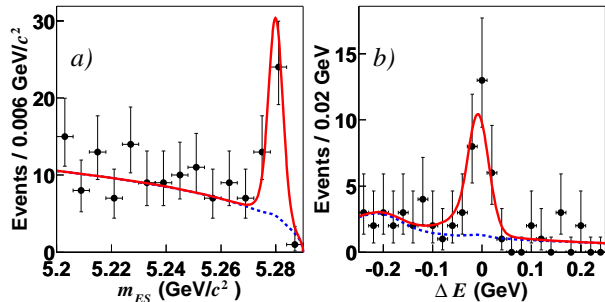
has a larger expected branching fraction, was not significant with those data samples.

The $B \rightarrow K^{(*)}\ell^+\ell^-$ signal is identified with M_{bc} , ΔE (and $M(K\pi)$ for $K^*\ell^+\ell^-$). There are five types of background that may contribute. 1) Charmonium decays, $B \rightarrow J/\psi K^{(*)}$ and $\psi' K^{(*)}$ have to be removed by the corresponding $M(\ell^+\ell^-)$ veto windows around J/ψ and ψ' masses. Especially for e^+e^- modes, bremsstrahlung has to be taken into account. 2) Hadronic decays, $B \rightarrow K^{(*)}\pi^+\pi^-$, are almost completely removed by lepton selection criteria including minimum lepton momentum requirements, but the remaining small contribution has to be evaluated and subtracted from the signal peak. 3) Two leptons from semi-leptonic decays, either in the cascade $b \rightarrow c \rightarrow s, d$ chain or from two B mesons, combined with a random K^* . This is the dominant combinatorial background that can be reduced for example by using the missing energy of the event. 4) Continuum background, which can be reduced by shape variables. 5) Rare backgrounds, $K^*\gamma$ with a photon conversion to e^+e^- , and $K^{(*)}\pi^0$ with a π^0 decaying into $e^+e^- \gamma$. This background can be removed by requiring a minimum e^+e^- mass as is done by Belle or can be subtracted from the signal as done by BaBar.

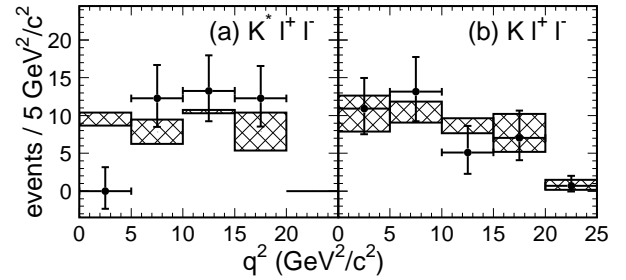
Belle has updated the analysis using a 140 fb⁻¹ data sample, with a number of improvements in the analysis procedure.³⁸ The most significant improvement is the lowered minimum lepton momentum of 0.7 (0.4) GeV for muons (electrons) from 1.0 (0.5) GeV to gain 12% (7%) in the total efficiency. In addition, a $K^*\ell^+\ell^-$ combination is removed if there can be an unobserved photon along with one of the leptons that can form $B \rightarrow J/\psi K \rightarrow \ell^+\ell^- \gamma K$. As a result, the first $B \rightarrow K^*\ell^+\ell^-$ signal is observed with a statistical significance of 5.7 from a fit to M_{bc} , as shown in Fig. 10, together with the improved $B \rightarrow K\ell^+\ell^-$ signal with a significance of 7.4.

BaBar has also updated the analysis using a 113 fb⁻¹ data sample,³⁹ with improvements such as the bremsstrahlung photon recovery to include $K^{(*)}e^+e^- \gamma$ events in the $K^{(*)}e^+e^-$ signal. Evidence for the $B \rightarrow K^*\ell^+\ell^-$ signal is also seen with a statistical significance of 3.3 from a simultaneous fit to M_{bc} , ΔE and $M(K\pi)$ (Fig. 11 shows their projections). A signal for $B \rightarrow K\ell^+\ell^-$ is clearly observed with a significance of ~ 8 (Fig. 12).

The branching fractions obtained are summa-

Figure 10. $B \rightarrow K^{(*)}\ell^+\ell^-$ signal observed by Belle.Figure 11. Evidence for $B \rightarrow K^*\ell^+\ell^-$ from BaBar.Figure 12. Signal for $B \rightarrow K\ell^+\ell^-$ from BaBar.Table 5. $B \rightarrow K^{(*)}\ell^+\ell^-$ branching fractions.

Mode	Belle (140 fb ⁻¹) [$\times 10^{-7}$]	BaBar (113 fb ⁻¹) [$\times 10^{-7}$]
$B \rightarrow Ke^+e^-$	$4.8^{+1.5}_{-1.3} \pm 0.3 \pm 0.1$	$7.9^{+1.9}_{-1.7} \pm 0.7$
$B \rightarrow K\mu^+\mu^-$	$4.8^{+1.3}_{-1.1} \pm 0.3 \pm 0.2$	$4.8^{+2.5}_{-2.0} \pm 0.4$
$B \rightarrow K\ell^+\ell^-$	$4.8^{+1.0}_{-0.9} \pm 0.3 \pm 0.1$	$6.9^{+1.5}_{-1.3} \pm 0.6$
$B \rightarrow K^*e^+e^-$	$14.9^{+5.2+1.1}_{-4.6-1.3} \pm 0.3$	$10.0^{+5.0}_{-4.2} \pm 1.3$
$B \rightarrow K^*\mu^+\mu^-$	$11.7^{+3.6}_{-3.1} \pm 0.8 \pm 0.6$	$12.8^{+7.8}_{-6.2} \pm 1.7$
$B \rightarrow K^*\ell^+\ell^-$	$11.5^{+2.6}_{-2.4} \pm 0.7 \pm 0.4$	$8.9^{+3.4}_{-2.9} \pm 1.1$

Figure 13. q^2 distributions for $B \rightarrow K^{(*)}\ell^+\ell^-$ from Belle.

rized in Table 5. For the combined $B \rightarrow K^*\ell^+\ell^-$ results, $\mathcal{B}(B \rightarrow K^*\ell^+\ell^-) = \mathcal{B}(B \rightarrow K^*\mu^+\mu^-) = 0.75\mathcal{B}(B \rightarrow K^*e^+e^-)$ is assumed which compensates the enhancement at the $q^2 = 0$ pole that appears more significantly in $K^*e^+e^-$, using the expected SM ratio.⁴⁰ The measured branching fractions are in agreement with the SM, for example⁴⁰ $(3.5 \pm 1.2) \times 10^{-7}$ for $B \rightarrow K\ell^+\ell^-$ and $(11.9 \pm 3.9) \times 10^{-7}$ for $B \rightarrow K^*\ell^+\ell^-$. We note that the experimental errors are already much smaller than the uncertainties in the SM predictions⁴¹ and the variations due to different model-dependent assumptions used to account for the hadronic uncertainties.

It is still too early to fit the q^2 distribution to constrain new physics. First attempts to extract the q^2 distribution using the individual M_{bc} signal yields in q^2 bins has been performed by Belle as shown in Fig. 13.

3.2 Measurement of $B \rightarrow X_s\ell^+\ell^-$

The first measurements of the $B \rightarrow K^{(*)}\ell^+\ell^-$ branching fractions are consistent with the SM predictions. However since these predictions have uncertainties that are already larger than the measurement errors, the inclusive rate for $B \rightarrow X_s\ell^+\ell^-$ be-

Table 6. $B \rightarrow X_s \ell^+ \ell^-$ branching fractions.

Mode	Belle (60 fb ⁻¹)	BaBar (78 fb ⁻¹)
	[$\times 10^{-6}$]	[$\times 10^{-6}$]
$X_s e^+ e^-$	$5.0 \pm 2.3^{+1.3}_{-1.1}$	$6.6 \pm 1.9^{+1.9}_{-1.6}$
$X_s \mu^+ \mu^-$	$7.9 \pm 2.1^{+2.1}_{-1.5}$	$5.7 \pm 2.8^{+1.7}_{-1.4}$
$X_s \ell^+ \ell^-$	$6.1 \pm 1.4^{+1.4}_{-1.1}$	$6.3 \pm 1.6^{+1.8}_{-1.5}$

comes more important in terms of the search for a deviation from the SM. In contrast to $B \rightarrow X_s \gamma$, the lepton pair alone does not provide a sufficient constraint to suppress the largest background from semi-leptonic decays. Therefore, it is only possible to use the semi-inclusive method to sum up the exclusive modes for now.

Belle has successfully measured the inclusive $B \rightarrow X_s \ell^+ \ell^-$ branching fraction⁴² from a 60 fb⁻¹ data sample by applying the method to sum up the X_s final state with one kaon (K^+ or K_S^0) and up to four pions, of which one pion is allowed to be π^0 . Assuming the K_L^0 contribution is the same as K_S^0 , this set of final states covers $82 \pm 2\%$ of the signal. In addition, $M(X_s)$ is required to be below 2.1 GeV in order to reduce backgrounds. For leptons, minimum momentum of 0.5 GeV for electrons, 1.0 GeV for muons and $M(\ell^+ \ell^-) > 0.2$ GeV are required. Background sources and the suppression techniques are similar to the exclusive decays.

A new result is reported by BaBar with a 78 fb⁻¹ data sample, using the same method with slightly different conditions.⁴³ BaBar includes up to two pions, corresponding to 75% of the signal, and require $M(X_s) < 1.8$ GeV. The minimum muon momentum requirement of 0.8 GeV is lower than Belle's.

The signal of 60 ± 14 events from Belle with a statistical significance of 5.4 is shown in Fig. 14, and 41 ± 10 events from BaBar with a significance of 4.6 is shown in Fig. 15. Corresponding branching fractions are very close to each other as given in Table 6, whose average is

$$\mathcal{B}(B \rightarrow X_s \ell^+ \ell^-) = (6.2 \pm 1.1^{+1.6}_{-1.3}) \times 10^{-6}. \quad (13)$$

The branching fraction results are for the dilepton mass range above $M(\ell^+ \ell^-) > 0.2$ GeV and are interpolated in the J/ψ and ψ' regions that are removed from the analysis, assuming no interference with these charmonium states.

The results may be compared with the SM prediction³⁴ of $(4.2 \pm 0.7) \times 10^{-6}$ integrated over the

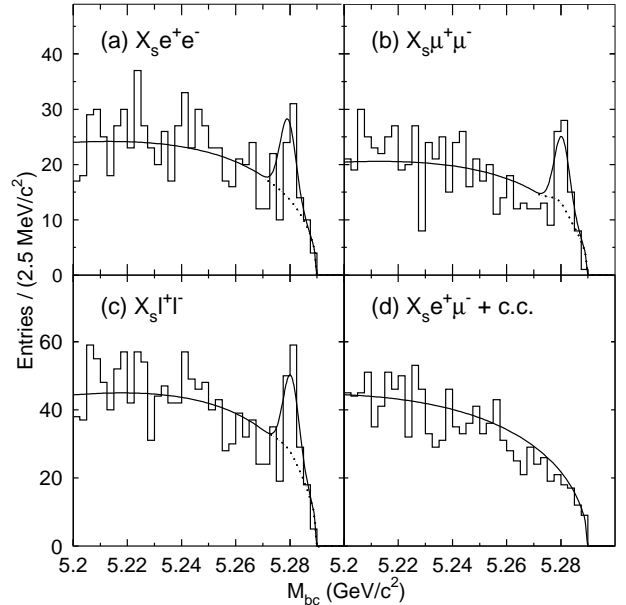


Figure 14. $B \rightarrow X_s \ell^+ \ell^-$ signal measured from Belle. The $X_s e^+ \mu^-$ sample, which is prohibited in the SM, represents the combinatorial backgrounds.

same dilepton mass range of $M(\ell^+ \ell^-) > 0.2$ GeV. With this requirement, the effect of the $q^2 = 0$ pole becomes insignificant, giving almost equal branching fractions for the electron and muon modes. The measured branching fractions are in agreement with the SM, considering the large measurement error. It should be noted that the large systematic error is dominated by the uncertainty in the $M(X_s)$ distribution, in particular the fraction of $B \rightarrow K^{(*)} \ell^+ \ell^-$, that will be reduced with more statistics. Distributions for $M(X_s)$ and $M(\ell^+ \ell^-)$ are shown in Figs. 16 and 17, in which no significant deviation from the SM is observed.

3.3 Search for $B \rightarrow K \nu \bar{\nu}$

The $b \rightarrow s \nu \bar{\nu}$ channel is sensitive to the weak-boson part of the $b \rightarrow s \ell^+ \ell^-$ amplitude, and does not involve the $q^2 = 0$ pole and interfering charmonium decays. It is experimentally challenging even for the easiest exclusive $B^+ \rightarrow K^+ \nu \bar{\nu}$ channel, because there is only one measurable kaon track out of the three-body final state that characterize the signal. In order to identify the signal, the other side B decay has to be tagged, so that there is only one kaon in the rest of the event. The search is attempted by BaBar using two techniques to tag the other B .

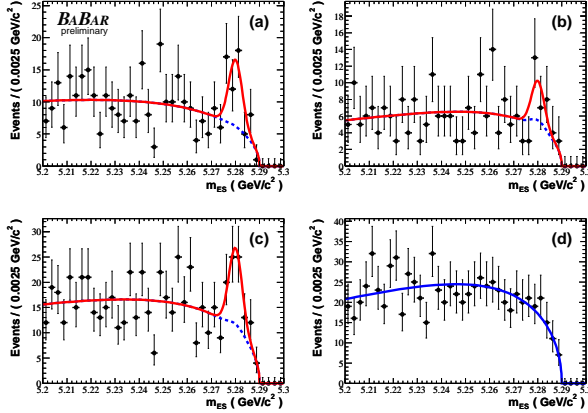


Figure 15. (a) $B \rightarrow X_s e^+ e^-$, (b) $B \rightarrow X_s \mu^+ \mu^-$, (c) $B \rightarrow X_s \ell^+ \ell^-$ signals with the (d) $X_s e^+ \mu^-$ sample from BaBar.

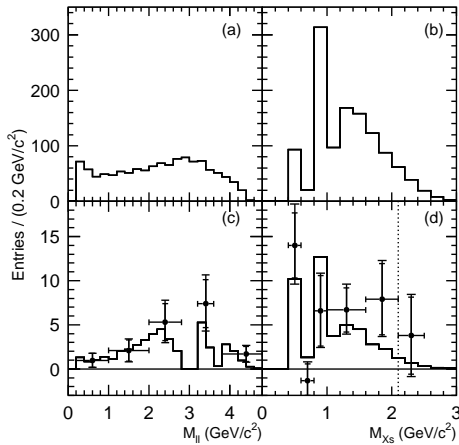


Figure 16. $M(\ell^+ \ell^-)$ (left) and $M(X_s)$ (right) distributions for $B \rightarrow X_s \ell^+ \ell^-$ from Belle (points with error bars), compared with the SM predictions before (top) and after (bottom) including detector acceptance effects.

One method⁴⁴ is to require a D^0 meson and a lepton in the event that come from the $B^- \rightarrow D^{(*)0} \ell^- \bar{\nu}$ decay channel to tag the semi-leptonic decay of the other side B . After removing the signal kaon and the tag-side D^0 and lepton, there should be no remaining charged tracks, and the energy in the calorimeter should be at most that from the disregarded soft photon or π^0 from the D^{*0} decay. The signal window is defined in the plane of the remaining energy (less than 0.5 GeV) and the reconstructed D^0 mass (within $\pm 3\sigma$). Two candidates are found using a 51 fb^{-1} data sample (Fig. 18) with a tagging efficiency of 0.5%, where 2.2 background events are expected. This leads to the upper limit

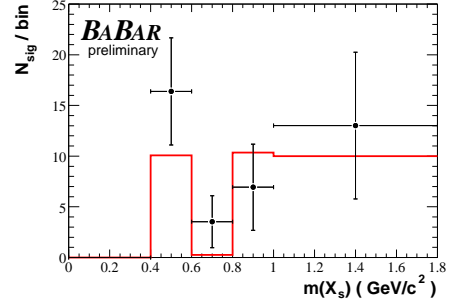


Figure 17. $M(X_s)$ distribution for $B \rightarrow X_s \ell^+ \ell^-$ from BaBar.

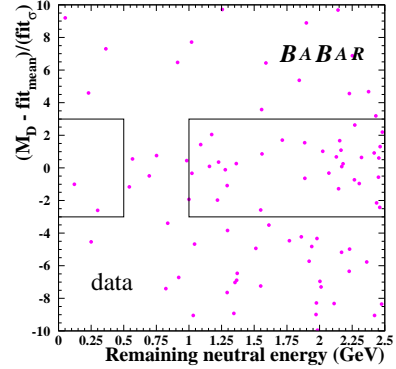


Figure 18. $B \rightarrow K \nu \bar{\nu}$ search results from BaBar using the semi-leptonic tag technique.

of $\mathcal{B}(B \rightarrow K \nu \bar{\nu}) < 9.4 \times 10^{-5}$ at the 90% confidence level.

The other method⁴⁵ is to require a full reconstruction of the hadronic decay $B^- \rightarrow D^0 X^-$, where X^- represents a combination of up to three charged pions or kaons and up to two π^0 with a net charge of -1 to tag the hadronic decay of the other side B . In this case, the maximum remaining energy is reduced to 0.3 GeV. The signal is identified with a high energy kaon with more than 1.5 GeV. Three candidates are found using a 80 fb^{-1} data sample with a tagging efficiency of 0.13%, where 2.7 ± 0.8 background events are expected. This leads to the upper limit of $\mathcal{B}(B \rightarrow K \nu \bar{\nu}) < 10.5 \times 10^{-5}$ at the 90% confidence level.

Since the two methods use statistically independent sub-samples, the two results can be combined to improve the upper limit as

$$\mathcal{B}(B \rightarrow K \nu \bar{\nu}) < 7.0 \times 10^{-5} \text{ (90\% C.L.)}, \quad (14)$$

which is still an order of magnitude higher than the SM prediction⁴⁶ of $\mathcal{B}(B \rightarrow K \nu \bar{\nu}) = (3.8^{+1.2}_{-0.6}) \times 10^{-6}$.

4 Pure Leptonic B Decays

Leptonic two-body B decays are highly helicity suppressed in the SM due to the large energy release from the B meson decaying into much lighter leptons. The branching fraction for $B^+ \rightarrow \ell^+ \nu$ is written down as

$$\mathcal{B}(B^+ \rightarrow \ell^+ \nu) = \frac{G_F^2 m_B}{8\pi} m_\ell^2 \left(1 - \frac{m_\ell^2}{m_B^2}\right)^2 f_B |V_{ub}|^2 \tau_B \quad (15)$$

which is sensitive to V_{ub} and the B meson decay constant f_B . The experimental sensitivities are still far above the predicted SM branching fractions.

However, if there is a non-SM decay amplitude that is not helicity suppressed, the branching fraction may be accessible by the on-going experiments. The decay modes considered are: $B^+ \rightarrow \tau^+ \nu$, $B^+ \rightarrow \mu^+ \nu$, $B_d^0 \rightarrow \mu^+ \mu^-$, $B_d^0 \rightarrow e^+ e^-$ and $B_s^0 \rightarrow \mu^+ \mu^-$. The lepton flavor violating $B_d^0 \rightarrow e^\pm \mu^\mp$ is also searched for.

4.1 Search for $B \rightarrow \tau \nu$ and $B \rightarrow \mu \nu$

The decay $B^+ \rightarrow \tau^+ \nu$ has been searched for by BaBar using 81 fb^{-1} of data. As there are at least two missing neutrinos, the same two techniques for the $B \rightarrow K \nu \bar{\nu}$ search are applied to tag the other side B using semi-leptonic decays and hadronic decays.

In the analysis with the leptonic tag, $\tau^+ \rightarrow e^+ \nu_e \bar{\nu}_\tau$ and $\mu^+ \nu_\mu \bar{\nu}_\tau$ are used.⁴⁷ A fit to the remaining energy, that can include a soft γ/π^0 in the other side B , shows no significant excess above the expected background (Fig. 19). The upper limit is obtained to be $\mathcal{B}(B^+ \rightarrow \tau^+ \nu) < 7.7 \times 10^{-4}$ at the 90% confidence level.

In the analysis with the hadronic tag, hadronic τ decays into $\pi^+ \bar{\nu}_\tau$, $\pi^+ \pi^0 \bar{\nu}_\tau$ and $\pi^+ \pi^- \pi^+ \bar{\nu}_\tau$ are also included.⁴⁸ The number of events with the remaining energy less than $\sim 100 \text{ MeV}$ is counted. In total 35 candidates are found for the expected background of $37.6 \pm 4.7 \pm 1.3$ events. The upper limit is obtained to be $\mathcal{B}(B^+ \rightarrow \tau^+ \nu) < 4.9 \times 10^{-4}$ at the 90% confidence level.

These two samples are combined to improve the upper limit,

$$\mathcal{B}(B^+ \rightarrow \tau^+ \nu_\tau) < 4.1 \times 10^{-4} \text{ (90\% CL)}. \quad (16)$$

This improves the previous upper limit given by L3.⁴⁹ The corresponding SM prediction is 7.5×10^{-5} for $\tau_B = 1.674 \text{ ps}$, $f_B = 198 \text{ MeV}$ and $|V_{ub}| = 0.0036$.

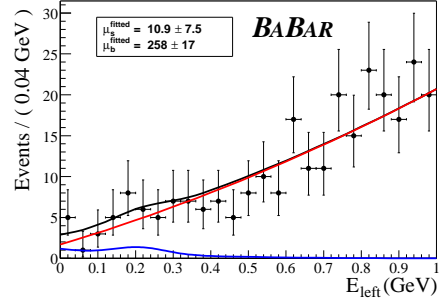


Figure 19. $B^+ \rightarrow \tau^+ \nu$ search results from BaBar using the semi-leptonic tag technique.

The decay $B^+ \rightarrow \mu^+ \nu$ has been searched for by Belle⁵⁰ and BaBar.⁵¹ The analysis technique is to use the “neutrino reconstruction” technique, to determine the neutrino momentum from the missing momentum of the event. The muon momentum is monochromatic, except for the small initial B meson momentum of 340 MeV , while the muon from the dominant background source of semi-leptonic B decays have a smaller momentum. No significant signal excess has been observed; the most stringent upper limit is given by BaBar using 81 fb^{-1} ,

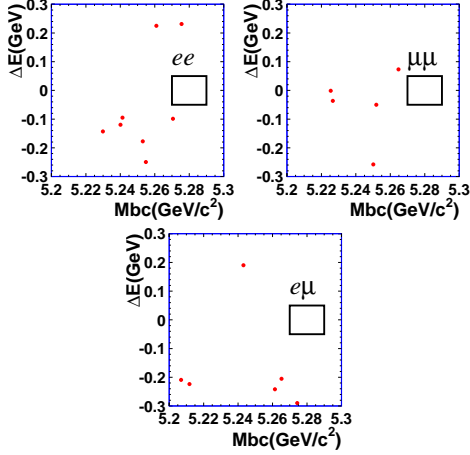
$$\mathcal{B}(B^+ \rightarrow \tau^+ \nu_\tau) < 6.6 \times 10^{-6} \text{ (90\% CL)}. \quad (17)$$

The SM predicts an order of magnitude smaller branching fraction of $\sim 4 \times 10^{-7}$.

4.2 Search for $B \rightarrow \ell^+ \ell^-$

In the SM, the decay $B_{d,s}^0 \rightarrow \ell^+ \ell^-$ occurs through the electroweak penguin transition $b \rightarrow (d, s) \ell^+ \ell^-$, and due to the helicity suppression, the expected branching fraction is extremely small:⁵² $(2.34 \pm 0.33) \times 10^{-15}$ for $B_d^0 \rightarrow e^+ e^-$, $(1.00 \pm 0.14) \times 10^{-10}$ for $B_d^0 \rightarrow \mu^+ \mu^-$ and $(3.4 \pm 0.5) \times 10^{-9}$ for $B_s^0 \rightarrow \mu^+ \mu^-$. The decay amplitude may be significantly enhanced in some extensions to the SM. For example, these decays are sensitive to the chirality flipping interaction in models with two Higgs doublets, and the branching fractions can be three orders of magnitude larger than the SM at large $\tan \beta$, and may be accessible by the B -factories for B_d^0 decays and by the Tevatron for B_s^0 decays. In this case the $B \rightarrow X_s \ell^+ \ell^-$ decay rate may not be affected and can be consistent with the SM. The search can be easily extended to the lepton flavor violating decay $B_d^0 \rightarrow e^\pm \mu^\mp$.

Belle has searched for the the decays $B_d^0 \rightarrow$

Figure 20. $B_d^0 \rightarrow \ell^+ \ell^-$ search results from Belle.

e^+e^- , $B_d^0 \rightarrow \mu^+\mu^-$ and $B_d^0 \rightarrow e^\pm\mu^\mp$, using a 78 fb^{-1} data sample.⁵³ The analysis method is similar to those for the other exclusive decays. The dominant background source is the continuum $e^+e^- \rightarrow c\bar{c}$ production in which both charm quarks decay into leptons. Leptons from $e^+e^- \rightarrow \tau^+\tau^-$ and two-photon processes can be removed by requiring five or more charged tracks in a event. No event was observed (Fig. 20) for the expected background events of 0.2 to 0.3, and the upper limits set are

$$\begin{aligned} \mathcal{B}(B_d^0 \rightarrow e^+e^-) &< 1.9 \times 10^{-7} \\ \mathcal{B}(B_d^0 \rightarrow \mu^+\mu^-) &< 1.6 \times 10^{-7} \\ \mathcal{B}(B_d^0 \rightarrow e^\pm\mu^\mp) &< 1.7 \times 10^{-7} \end{aligned} \quad (18)$$

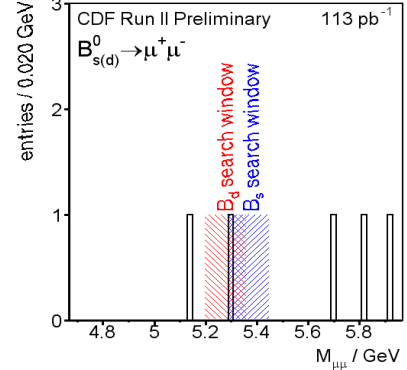
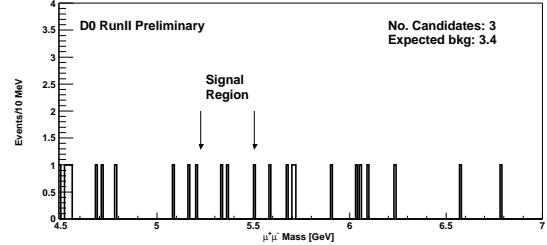
at the 90% confidence level.

For the B_s^0 decays, 113 pb^{-1} and 100 pb^{-1} of Run-II data from CDF and D0 respectively have been analyzed. Both analyses require three variables to reduce backgrounds and search for the signal in the $\mu^+\mu^-$ mass distribution. CDF uses the proper lifetime $c\tau$, the direction difference in azimuthal angle between the $\mu^+\mu^-$ vertex and momentum directions $\Delta\Phi$, and a measure of isolation of the B_s^0 candidate based on the tracks inside the cone around the B_s^0 direction; D0 also uses a similar set of variables.

CDF and D0 find one and three candidates as shown in Figs. 21 and 22, respectively. The CDF result leads to the upper limit of

$$\mathcal{B}(B_s^0 \rightarrow \mu^+\mu^-) < 9.5 \times 10^{-7} \quad (90\% \text{ CL}) \quad (19)$$

that supersedes the previous CDF Run-I result. D0's limit is $\mathcal{B}(B_s^0 \rightarrow \mu^+\mu^-) < 16 \times 10^{-7}$. CDF also re-

Figure 21. $B_s^0 \rightarrow \mu^+\mu^-$ search results from CDF.Figure 22. $B_s^0 \rightarrow \mu^+\mu^-$ search results from D0.

ports $\mathcal{B}(B_d^0 \rightarrow \mu^+\mu^-) < 2.5 \times 10^{-7}$, which is already competitive with Belle's result.

5 Conclusion

Figure 23 shows the currently measured branching fractions and upper limits for the rare B decays that involve a photon or a lepton pair. Most of the results have been updated rapidly along with the accumulation of the B -factory data: new modes and measurements in the exclusive $b \rightarrow s\gamma$ channels, new measurement of the CP-asymmetry in $B \rightarrow X_s\gamma$, the first observation of $B \rightarrow K^*\ell^+\ell^-$ by Belle and evidence from BaBar, new results on $B \rightarrow X_s\ell^+\ell^-$ from BaBar in agreement with Belle's, and new limits on $B \rightarrow K\nu\bar{\nu}$ and pure leptonic decays from BaBar, Belle and CDF are included. So far none of these results indicate a deviation from the SM. As $B \rightarrow K^*\ell^+\ell^-$ is finally measured, the next target will be the $b \rightarrow d\gamma$ transition in the decay $B \rightarrow \rho\gamma$.

There are still many programs to be pursued using these already observed rare B decay channels, in addition to the searches for unobserved modes. One

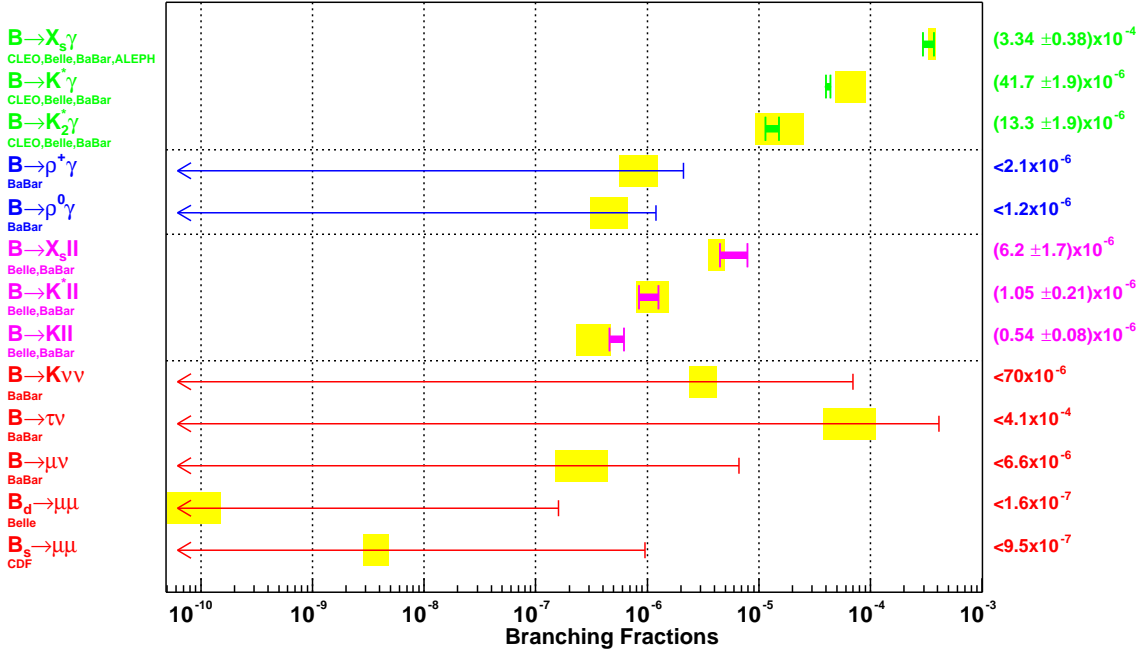


Figure 23. Summary of branching fractions and upper limits compared with the corresponding SM predictions.

example is a measurement for mixing-induced CP-violation in $b \rightarrow s\gamma$, for example with $B \rightarrow K^{*0}\gamma \rightarrow K_S^0\pi^0\gamma$. This channel has been considered to be experimentally challenging due to the displaced K_S^0 decay vertex; however, BaBar has recently demonstrated that it is possible to measure the B decay vertex from K_S^0 in the $B^0 \rightarrow K_S^0\pi^0$ channel,⁵⁴ and the same technique is applicable to $B \rightarrow K^*\gamma$. The other example is the measurement of the forward-backward asymmetry in $B \rightarrow K^*\ell^+\ell^-$ or $B \rightarrow X_s\ell^+\ell^-$. These examples demand an order of magnitude larger data sample than is available. Fortunately, Belle and BaBar are still collecting more data with improved luminosities expected, and are planning to extend their luminosities by orders of magnitude.

Acknowledgments

I wish to thank all the members of the Belle collaboration, Jeff Richman, Stephane Willocq and Mark Convery for providing the latest BaBar results, Rich Galik for the CLEO results, Majorie Shapiro for the CDF results, Brad Abbott and Vivek Jain for the D0 results, and Paoti Chang, Jim Alexander and Jim Smith of the Heavy Flavor Averaging Group for the averaged numbers from the last minute results. I acknowledge Enrico Lunghi and Mikolaj Misiak

among many theorists for many useful private discussions. I have to note that all the progress would not have been possible at all without excellent accelerator performances by the KEKB and PEP-II accelerator teams. Last but not least, I would like to thank the Lepton-Photon '03 organizers for all their efforts in the excellent conference organization.

References

1. Belle Collaboration, K. Abe *et al.*, arXiv:hep-ex/0308035.
2. CLEO Collaboration, S. Chen *et al.*, *Phys. Rev. Lett.* **87**, 251807 (2001).
3. ALEPH Collaboration, R. Barate *et al.*, *Phys. Lett. B* **429**, 169 (1998).
4. Belle Collaboration, K. Abe *et al.*, *Phys. Lett. B* **511**, 151 (2001).
5. BaBar Collaboration, B. Aubert *et al.*, arXiv:hep-ex/0207076.
6. BaBar Collaboration, B. Aubert *et al.*, arXiv:hep-ex/0207074.
7. C. Jessop, SLAC-PUB-9610 (2002).
8. P. Gambino and M. Misiak, *Nucl. Phys. B* **611**, 338 (2001).
9. K. Chetyrkin, M. Misiak and M. Münz, *Phys. Lett. B* **400**, 206 (1997), Erratum *ibid.* **425**, 414 (1998); A. Kagan and M. Neubert, *Eur. Phys. J. C* **7**, 5 (1999).
10. F. Borzumati, C. Greub, *Phys. Rev. D* **58**, 074004 (1998)

11. For example, M. Ciuchini, G. Degrossi, P. Gambino and G. F. Giudice, *Nucl. Phys. B* **534**, 3 (1998); C. Bobeth, M. Misiak and J. Urban, *Nucl. Phys. B* **567**, 153 (2000); M. Carena, D. Garcia, U. Nierste and C. Wagner, *Phys. Lett. B* **499**, 141 (2001).
12. CLEO Collaboration, T. E. Coan *et al.*, *Phys. Rev. Lett.* **84**, 5283 (2000).
13. BaBar Collaboration, B. Aubert *et al.*, *Phys. Rev. Lett.* **88**, 101905 (2002).
14. Belle Collaboration, K. Abe *et al.*, Belle-CONF-0319.
15. S. Bosch and G. Buchalla, *Nucl. Phys. B* **621**, 459 (2002); A. Ali and A. Parkhomenko, *Eur. Phys. J. C* **23**, 89 (2002).
16. D. Becirevic, arXiv:hep-ph/0211340; D. Becirevic, talk given at Ringberg Phenomenology Workshop on Heavy Flavours, Rottach-Egern, Germany, April 27 - May 2, 2003.
17. A. Kagan and M. Neubert, *Phys. Lett. B* **539**, 227 (2002).
18. D. Atwood, M. Gronau and A. Soni, *Phys. Rev. Lett.* **79**, 185 (1997).
19. M. Gronau, Y. Grossman, D. Pirjol and A. Ryd, *PRL* **88**, 051802 (2002).
20. Belle Collaboration, S. Nishida *et al.*, *PRL* **89**, 231801 (2002).
21. BaBar Collaboration, B. Aubert *et al.*, arXiv:hep-ex/0308021.
22. S. Veseli and M. G. Olsson, *Phys. Lett. B* **367**, 309 (1996)
23. Belle Collaboration, A. Drutskoy *et al.*, arXiv:hep-ex/0309006.
24. CLEO Collaboration, K. Edwards *et al.*, *Phys. Rev. D* **68**, 011102 (2003)
25. J. Soares, *Nucl. Phys. B* **367**, 575 (1991).
26. A. Kagan and M. Neubert, *Phys. Rev. D* **58**, 094012 (1998).
27. K. Kiers, A. Soni and G. Wu, *Phys. Rev. D* **62**, 116004 (2000); S. Baek and P. Ko, *Phys. Rev. Lett.* **83**, 488 (1998).
28. CLEO Collaboration, T. Coan *et al.*, *PRL* **86**, 5661 (2001).
29. Belle Collaboration, K. Abe *et al.*, arXiv:hep-ex/0308038.
30. BaBar Collaboration, B. Aubert *et al.*, arXiv:hep-ex/0306038.
31. M. Nakao for the Belle Collaboration, talk given at 2nd Workshop on the CKM Unitarity Triangle, Durham, England, Apr. 2003, arXiv:hep-ex/0307031.
32. T. Hurth and E. Lunghi, arXiv:hep-ex/0307142.
33. C. Bobeth, M. Misiak and J. Urban, *Nucl. Phys. B* **574**, 291 (2000); H. H. Asatrian, H. M. Asatrian, C. Greub and M. Walker, *Phys. Lett. B* **507**, 162 (2001); H. H. Asatrian, H. M. Asatrian, C. Greub and M. Walker, *Phys. Rev. D* **65**, 074004 (2002).
34. A. Ali, E. Lunghi, C. Greub and G. Hiller, *PRD* **66**, 034002 (2002).
35. For example, E. Lunghi, A. Masiero, I. Scimemi and L. Silverstrini, *Nucl. Phys. B* **568**, 120 (2000); J. L. Hewett and J. D. Wells, *Phys. Rev. D* **55**, 5549 (1997); T. Goto, Y. Okada, Y. Shimizu and M. Tanaka, *Phys. Rev. D* **55**, 4273 (1997); G. Burdman, *Phys. Rev. D* **52**, 6400 (1995); N. G. Deshpande, K. Panose and J. Trampetić, *Phys. Lett. B* **308**, 322 (1993); W. S. Hou, R. S. Willey and A. Soni, *Phys. Rev. Lett.* **58**, 1608 (1987).
36. Belle Collaboration, K. Abe *et al.*, *Phys. Rev. Lett.* **88**, 021801 (2002).
37. BaBar Collaboration, B. Aubert *et al.*, arXiv:hep-ex/0207082.
38. Belle Collaboration, A. Ishikawa *et al.*, arXiv:hep-ex/0308044.
39. BaBar Collaboration, B. Aubert *et al.*, arXiv:hep-ex/0308042.
40. A. Ali, E. Lunghi, C. Greub and G. Hiller, *Phys. Rev. D* **66**, 034002 (2002); E. Lunghi, arXiv:hep-ph/0210379.
41. For example, D. Melikhov, N. Nikitin and S. Simula, *Phys. Lett. B* **410**, 290 (1997); P. Colangelo, F. De Fazio, P. Santorelli and E. Scrimieri, *Phys. Rev. D* **53**, 3672 (1996), Erratum-ibid. *D* **57**, 3186 (1998); M. Zhong, Y. L. Wu and W. Y. Wang, *Int. J. Mod. Phys. A* **18**, 1959 (2003); A. Faessler *et al.*, *Eur. Phys. J. direct C* **4**, 18 (2002); T. M. Aliev, C. S. Kim and Y. G. Kim, *Phys. Rev. D* **62**, 014026 (2000); W. Jaus and D. Wyler, *Phys. Rev. D* **41**, 3405 (1990).
42. Belle Collaboration, J. Kaneko *et al.*, *Phys. Rev. Lett.* **90**, 021801 (2003).
43. BaBar Collaboration, B. Aubert *et al.*, arXiv:hep-ex/0308016.
44. BaBar Collaboration, B. Aubert *et al.*, arXiv:hep-ex/0207069.
45. BaBar Collaboration, B. Aubert *et al.*, arXiv:hep-ex/0304020.
46. G. Buchalla, G. Hiller and G. Isidori, *Phys. Rev. D* **63**, 014015 (2001).
47. BaBar Collaboration, B. Aubert *et al.*, arXiv:hep-ex/0303034.
48. BaBar Collaboration, B. Aubert *et al.*, arXiv:hep-ex/0304030.
49. L3 Collaboration, M. Acciarri *et al.*, *Phys. Lett. B* **396**, 327 (1997).
50. Belle Collaboration, K. Abe *et al.*, Belle-CONF-0247.
51. BaBar Collaboration, B. Aubert *et al.*, arXiv:hep-ex/0307047.
52. A. Buras, *Phys. Lett. B* **566**, 115 (2003).
53. Belle Collaboration, M.-C. Chang *et al.*, arXiv:hep-ex/0309069.
54. T. Browder, talk given at XXI International Symposium on Lepton and Photon Interactions at High Energies, Batavia, Illinois, USA, Aug. 2003, in this Proceedings.